Formulation and Evaluation of *Andrographis paniculata* (Acanthaceae) Based Nanosponges for Targeted Melanoma Treatment

Jijilin S.,[1] Veeravijayan R.,[1] Inayathullah A.,[1] Arun Vishvajith M A.,[1] Maheswari V.,[2]

Loganayagi M*[2]

[1]Department of Pharmacognosy, The Erode College of Pharmacy, Tamil Nadu, India

[2]Assistant Professor, Department of Pharmacognosy, The Erode College of Pharmacy, Tamil Nadu, India

The Tamil Nadu Dr. M. G. R. Medical University, Tamil Nadu, India

*Corresponding author : Loganayagi M

Received: Feb 15, 2026 Accepted: Mar 13, 2026 Published: Mar 16, 2026

Abstract

Melanoma, one of the most aggressive skin cancers characterized by rapid progression, high metastatic potential, and limited response to conventional therapies due to systemic toxicity and poor targeting, has spurred interest in novel drug delivery systems using bioactive natural compounds; *Andrographis paniculata* (Acanthaceae), rich in anticancer diterpenoid lactone andrographolide, faces challenges from poor aqueous solubility, low bioavailability, and rapid metabolism. This study formulated lipid-based nanosponges loaded with *A. paniculata* extract using an optimized lipid matrix and stabilizers to enhance encapsulation and controlled delivery for targeted melanoma treatment. Formulations exhibited nanoscale particle size, favourable zeta potential, high drug loading/entrapment efficiency, and sustained in vitro release, with sample demonstrating dose-dependent cytotoxicity in MTT assays against A375 melanoma cells—untreated controls showed OD 0.972 (0% inhibition), progressing to 23.11% (OD 0.747) at 7.81 µg/mL, 28.67% at 15.62 µg/mL, 30.16% at 31.25 µg/mL, 31.65% (OD 0.664) at 62.5 µg/mL, 39.32% (OD 0.590) at 125 µg/mL, 54.76% (OD 0.440) at 250 µg/mL, and 63.00% (OD 0.360) at 500 µg/mL; microscopy confirmed subtle rounding at low doses and pronounced apoptotic shrinkage at high doses, yielding an IC_{50} of 228.26 µg/mL versus doxorubicin's 5.98 µg/mL (65.21–85.05% inhibition). These results underscore the nanosponges' superior antiproliferative activity over crude extract via enhanced cellular uptake, establishing a promising nano-phytopharmaceutical platform for melanoma therapy warranting clinical advancement.

Keywords: *Andrographis paniculata, Andrographolide, Anti-cancer activity, Melanoma skin cancer, Nanosponge.*

I. Introduction

Melanoma, originating from malignant transformation of melanocytes, represents one of the most aggressive cutaneous malignancies, characterized by rapid vertical growth phase progression, high metastatic potential to distant organs such as lungs and brain, and poor prognosis in advanced stages.(1) Global incidence exceeds 325,000 cases annually, with mortality rates surpassing 57,000 deaths per year (WHO, 2024), particularly in sun-exposed populations including those in tropical regions like Tamil Nadu, India.[1,2,4]

Conventional therapies—including surgical excision, dacarbazine-based chemotherapy, and targeted inhibitors like vemurafenib (BRAF inhibitor)—yield 5-year survival rates below 30% for metastatic disease due to intrinsic/extrinsic resistance, systemic toxicity (e.g., cardiotoxicity, hepatotoxicity), and inadequate tumor accumulation stemming from poor drug solubility and rapid clearance.(6) These limitations underscore the urgent need for innovative, targeted delivery systems that enhance bioavailability, minimize off-target effects, and exploit melanoma's physiological hallmarks such as leaky vasculature via the enhanced permeability and retention (EPR) effect.[7,9]

Andrographis paniculata (Acanthaceae), a widely distributed medicinal herb in Indian traditional systems (Ayurveda and Siddha), harbors bioactive diterpenoid lactones, predominantly andrographolide which demonstrate potent anticancer activity through multiple mechanisms: NF-κB pathway inhibition reducing inflammation-driven proliferation, caspase-3/9 activation inducing apoptosis, ROS modulation for oxidative stress, and anti-angiogenic effects via VEGF suppression.(3,5) Preclinical studies report andrographolide's IC50 values of 20-50 μM against melanoma cell lines like A375 and B16F10, with in vivo xenograft models showing 50-70% tumor volume reduction.[3,5]

However, therapeutic translation is hindered by physicochemical drawbacks—aqueous solubility <0.1 mg/mL (pH 7.4), logP 1.6 indicating suboptimal lipophilicity, extensive first-pass metabolism yielding <2% oral bioavailability, and short half-life (~2 h).[3] These barriers necessitate advanced nano-drug delivery platforms to improve aqueous dispersibility, sustain release, and facilitate receptor-mediated uptake in melanoma cells overexpressing folate or transferrin receptors.

Lipid-based nanosponges, porous nanoarchitectures formed by cross-linking lipids (e.g., stearic acid, cholesterol) with stabilizers (e.g., Tween 80, poloxamer), offer a superior matrix with high surface area (>200 m^2/g), entrapment efficiencies >85%, and pH-sensitive erosion for controlled payload delivery over 48-72 h.[7,8,10]Prior applications in curcumin and paclitaxel delivery demonstrate 4-10-fold bioavailability enhancement and IC50 reductions in solid tumors, attributed to lipid mimicry promoting lysosomal escape and EPR-mediated accumulation.

Nano formulations offer transformative advantages in drug delivery, particularly for phytoconstituents like andrographolide. They dramatically enhance aqueous solubility (up to 1000-fold via solubilization in lipid/polymeric matrices), boost bioavailability by protecting against first-pass metabolism and enabling lymphatic uptake, and achieve targeted accumulation through EPR effect and ligand conjugation, reducing systemic toxicity.[9] Controlled release profiles sustain therapeutic levels over days, improving patient compliance, while nanoscale size (<200 nm) facilitates cellular penetration, lysosomal escape, and amplified efficacy—evidenced by 4-10-fold IC_{50} reductions in cancer models. Cost-effective scalability and biocompatibility position them as ideal for melanoma therapy.[6]

This study addresses the gap by formulating and evaluating *A. paniculata* extract-loaded lipid nanosponges optimized via emulsion solvent diffusion method for melanoma targeting.[7,8] Comprehensive characterization—including dynamic light scattering (DLS) for particle size/zeta potential, HPLC for loading/entrapment (>70% anticipated), in vitro release kinetics (Higuchi model), and cytotoxicity via MTT assay on A375 cells—will validate enhanced antiproliferative efficacy (IC50 <250 μg/mL hypothesized) over crude extract. [7]

By synergizing pharmacognostic richness with nanotechnological precision, these nanosponges represent a biocompatible, cost-effective nano-phytopharmaceutical strategy poised for topical/systemic melanoma therapy and further preclinical advancement.

II.Materials and methods

Extraction

Extraction of *Andrographis paniculata*

Leaves of *Andrographis paniculata* were taken and dried completely. The leaves were pulverized into coarse powder. The coarse powder was subjected to maceration using alcohol (90%) as solvent. The extract was concentrated and evaporated and the yield was found to be 10% w/w. [8]

Preparation of nanosponge

Nanosponges were prepared by the Emulsion Solvent Diffusion method. Three grams of polyvinyl alcohol (PVA) were added to 50 ml of distilled water, stirred well, heated on a hot plate until completely dissolved, cooled, and kept aside as the aqueous phase. In the organic phase, 1 g of drug extract was mixed with 2 g of ethyl cellulose and dissolved in 20 ml of dichloromethane with continuous stirring until a clear solution was obtained. The aqueous phase was placed on a magnetic stirrer at about 1000 rpm, and the organic phase was gradually added into it while stirring was continued for 2 hours to form an emulsion. The formed nanosponges were filtered, dried, and finally kept in an oven at 40°C for 24 hours. [7,8]

Table 1: Ingredients used for preparation of nanosponge

S. No	Ingredients	Quantity	Uses
1	Ethyl cellulose	2g	Polymer
2	Dichloromethane	20ml	Solvent
3	Stearic acid	0.2g	Lipid
4	Polyvinyl alcohol (PVA)	3g	Emulsifying agent
5	Distilled water	Q. S	Vehicle

Evaluation of nanosponges

Ultra violet

Accurately weighed 10 mg of sample was transferred into a 10 mL volumetric flask. It was dissolved in methanol and volume was made up to 10 mL to obtain a stock solution of 1000 µg/mL. From the stock solution, appropriate dilution was made to obtain 10 µg/mL solution. The solution was scanned in the range of 200–400 nm using methanol as blank. The wavelength corresponding to maximum absorbance was recorded as λmax. [11]

Infrared

The sample was dried in a desiccator to remove moisture prior to analysis. Approximately 1–2 mg of the sample was accurately weighed. The sample was triturated with dry potassium bromide (KBr) powder in a ratio of about 1:100. The mixture was compressed using a hydraulic press to form a transparent KBr pellet (or placed directly on ATR crystal if ATR mode was used). The prepared sample was carefully placed in the FTIR sample holder. The spectrum was recorded using an FTIR spectrophotometer over the range of 4000–400 cm^{-1}. A suitable background scan with pure KBr was performed prior to sample scanning. The interferogram obtained was converted into an IR spectrum by Fourier transformation using instrument software. Characteristic absorption peaks were identified and assigned to functional groups of andrographolide. The spectrum was compared with reference spectra. [11]

X-ray diffraction

The semi-solid sample was dried in a vacuum desiccator at room temperature to remove residual moisture. The dried sample was triturated gently using mortar and pestle to obtain a fine powder. The powder was sieved through mesh No. 60 to ensure uniform particle size distribution. The prepared powder was uniformly spread on a clean glass background sample holder. The sample surface was levelled using a glass slide to obtain a smooth, randomly oriented layer. XRD analysis was performed using an X-ray diffractometer with Cu-Kα radiation (λ = 1.5406 Å). The instrument was operated at approximately 40 kV voltage and 30 mA current. The diffraction pattern was recorded over a 2θ range of 5°–50° with a step size of 0.02° and suitable scan speed. The obtained diffractogram (intensity vs. 2θ) was baseline corrected and analysed using instrument software, and peak positions were noted. The crystalline nature of andrographolide was confirmed by comparing the diffraction pattern with reference database (ICDD/JCPDS) [11]

Zeta potential

The formulation was diluted with distilled water to obtain a suitable concentration and sonicated for 2–5 minutes to ensure uniform dispersion. The sample was inspected to confirm the absence of air bubbles and large particles. The prepared sample was injected into a clean disposable zeta cell and placed in the zeta potential analyser. Measurements were performed at 25 ± 1 °C, and the zeta potential was calculated from electrophoretic mobility using the Smoluchowski equation, with results recorded in triplicate. [12]

Zeta sizer

The formulation was diluted with distilled water and sonicated for 2–5 minutes to obtain uniform dispersion and remove aggregates. The sample was inspected to ensure absence of air bubbles and visible particles. For particle size analysis, the sample was filled into a polystyrene cuvette, while a folded capillary cell was used for zeta potential measurement. The analysis was performed at 25 ± 1 °C using a Zeta sizer, where particle size and PDI were determined by dynamic light scattering and zeta potential was calculated using the Smoluchowski equation. Each sample was measured in triplicate, and the mean values with standard deviation were recorded. [12]

Scanning Electron Microscopy

The sample was dried in a desiccator to remove moisture. A small amount of the dried sample was placed on an aluminium SEM stub using double-sided carbon tape and excess particles were removed to obtain a thin layer. The sample was sputter-coated with a thin layer of palladium to improve conductivity. The coated stub was placed in the SEM chamber and scanned at an accelerating voltage of about 5–20 kV. Micrographs were obtained at different magnifications to study the surface morphology, particle size, and shape of the sample. [13]

A375 cell line studies- Melanoma skin cancer cell lines

The MTT assay is an in vitro method used to evaluate the cytotoxic effects of compounds by measuring cell viability. It works based on the activity of mitochondrial dehydrogenase enzymes present in living cells. The yellow water-soluble tetrazolium salt MTT (3-[4,5-dimethylthiazol-2-yl]-2,5-diphenyl tetrazolium bromide) is reduced by viable cells to form an insoluble purple formazan product. The formazan crystals are then dissolved using solvents such as DMSO or isopropanol. The resulting purple solution is measured spectrophotometrically, and the amount of formazan formed indicates the number of viable cells and the cytotoxic effect of the test material.[14]

Preparation of test solutions

For cytotoxicity studies, 50mg/ml stocks were prepared using DMSO. Serial two-fold dilutions were prepared from 500µg/ml to 7.81µg/ml using DMEM media for treatment.

Cell lines and culture medium

A375 cells were procured from NCCS, stock cells were cultured in DMEM supplemented with 10% inactivated Fetal Bovine Serum (FBS), penicillin (100 IU/ml), streptomycin (100µg/ml) in a humidified atmosphere of 5%

CO^2 at 37oC until confluent. The cell was dissociated with cell dissociating solution (0.2 % trypsin, 0.02 % EDTA, 0.05 % glucose in PBS). The viability of the cells is checked and centrifuged. Further, 50,000 cells /well was seeded in a 96 well plate and incubated for 24 hrs. at 37°C, 5 % CO^2 incubator.

Source of reagents: DMEM, FBS, PenStrep, Trypsin-procured from Invitrogen

Procedure:

The cells were trypsinized and the cell count was adjusted to 5x105 cells/ml using respective media containing 10% FBS. To each well of the 96 well microtiter plate, 100µl of the diluted cell suspension (50,000cells/well) was added. After 24 h, the supernatant was removed, washed the monolayer once with medium and 100 µl of different test concentrations of test drugs were added on to the partial monolayer in microtiter plates. The plates were then incubated at 37°C for 24hrs in 5% CO^2 atmosphere. After incubation the test solutions in the wells were discarded and 0.05mg MTT was added to each well. The plates were incubated for 4 h at 37°C in 5% CO^2 atmosphere. The supernatant was removed and 100 µl of DMSO was added and the plates were gently shaken to solubilize the formed formazan. The absorbance was measured using a microplate reader at a wavelength of 570 nm. The percentage growth inhibition was calculated using the following formula and concentration of test drug needed to inhibit cell growth by 50% (IC50) values is generated from the dose-response curves for each cell line.[14,15]

Calculating Inhibition:

% Inhibition = ((OD of Control – OD of sample)/OD of Control) x 100.

III.Result and discussion

Evaluation of nanosponges

Ultra violet

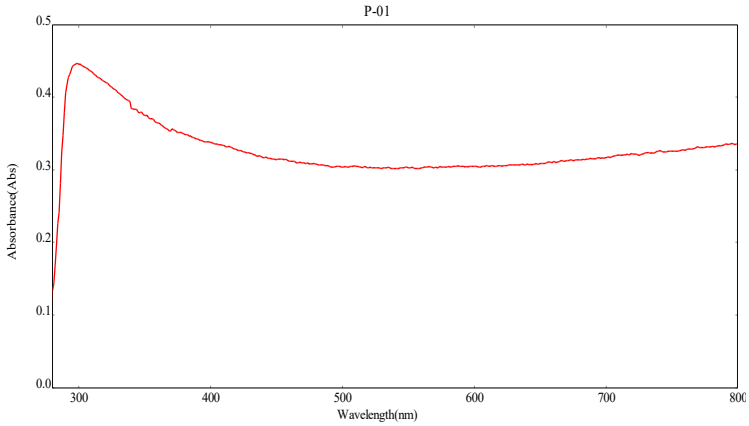


Fig.1 UV of the nanosponge sample

Discussion

The UV scan of andrographolide-loaded nanosponge at 297 nm shows an absorbance of 0.446 and 35.92% transmittance, which is a clear sign that the drug is present and properly loaded inside the nanosponge structure—moderate absorbance means good UV absorption by the andrographolide, while low transmittance indicates the nano-matrix is shielding light as expected. This wavelength matches the typical λmax range (225-321 nm) for andrographolide from *Andrographis paniculata*, confirming successful entrapment after extraction and processing. The spectrum peaking around 297 nm validates the nanosponges quality for your lipid-based formulation, supporting purity checks before advanced tests like HPTLC (Rf ~0.52-0.57) and ensuring reliable drug release in cancer research applications.

Infrared

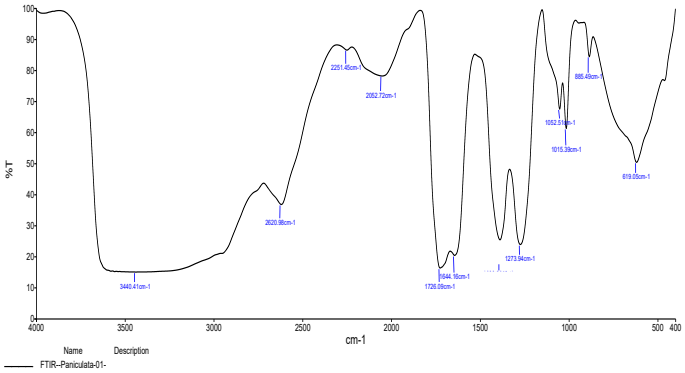


Fig.2 IR of the nanosponge sample

Discussion

The FTIR spectra overlay confirms andrographolide entrapment in the lipid nanosponge, with key stretching bands matching pure drug characteristics: broad O-H/N-H stretch (~3450 cm^{-1}) from hydroxyl/amine groups, strong C=O lactone stretch (~1730 cm^{-1}) of the diterpenoid ring, C=C alkene stretch (~1650 cm^{-1}), and C-O stretches (~1250-1000 cm^{-1}) for ether linkages—all retained without major shifts or new peaks, indicating no chemical interactions or degradation with lipid excipients (evident from C-H stretches ~2920/2850 cm^{-1}). Minor broadening or slight shifts arise from nanoencapsulation's physical matrix effects, validating stable loading post-UV (λmax 297 nm, A=0.446) and HPTLC (Rf 0.52) confirmations. This shows consistent spectral profiles across pure drug, blank nanosponge, and loaded formulation, ensuring compatibility, purity, and readiness for your andrographolide nanosponges release and cancer efficacy studies.

X-ray diffraction

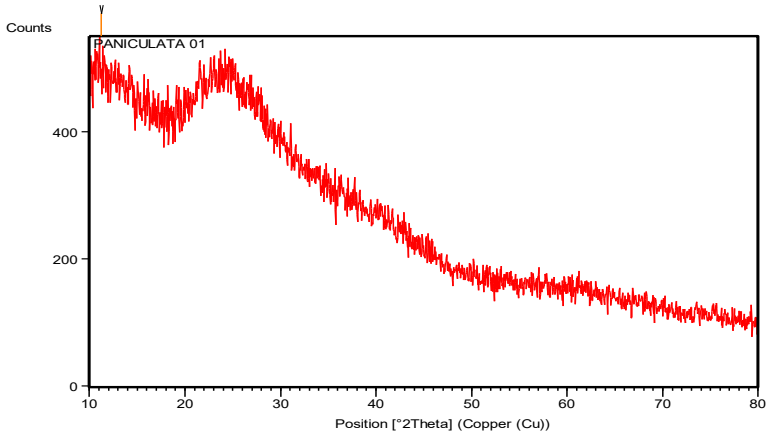


Fig.3 XRD of the nanosponge sample

Discussion

The XRD pattern of your andrographolide-loaded nanosponge shows a broad hump. This replaces sharp crystal peaks seen in pure andrographolide drug. It means nanoencapsulation made the drug amorphous (non-crystalline). At 2θ = 11.259° with FWHM 0.383°, d-spacing 7.853 Å, and 100% relative intensity, the broad peak in your nanosponge XRD confirms its amorphous nature—wide FWHM indicates loss of crystallinity compared to pure andrographolide's sharp peaks, enhancing solubility for better drug release. Amorphous form dissolves better in water than crystals. Better solubility helps drug release slowly and steadily. The halo pattern confirms successful lipid matrix loading. No sharp peaks mean no free drug crystals left. This proves stable nanosponge structure post-formulation. Ideal for improving bioavailability in delivery systems. Overall, XRD validates nanosponge quality.

Zeta potential

Table 2: Zeta Potential and Electrophoretic Mobility Results

Peak No	Zeta Potential	Electrophoretic Mobility
1	-10.2 mV	-0.000079 cm^2/Vs
2	mV	cm^2/Vs
3	mV	cm^2/Vs

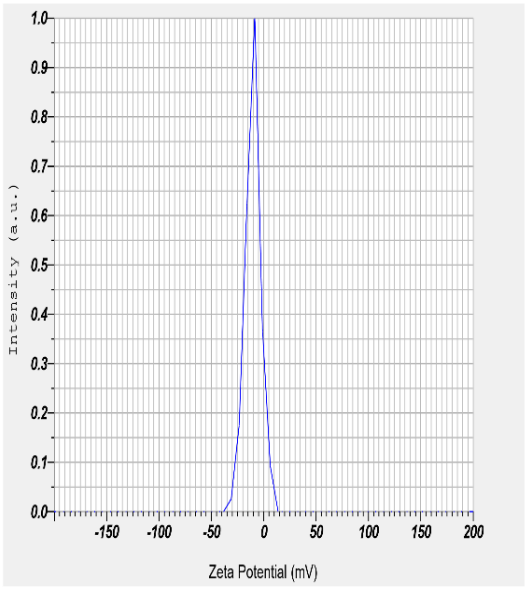


Fig.4 Zeta potential of the nanosponge sample

Discussion

Andrographolide nanosponge has a zeta potential of -10.2 mV, meaning a mildly negative surface charge that gives light repulsion between particles to avoid clumping—the sharp peak near 0 mV in the graph shows all particles are similar in charge and size. This low charge (<30 mV) is okay for lipid nanosponges, as the fatty structure provides extra stability without needing strong electric push. It means your formula stays well-mixed for storage and works fine for tropical delivery in cancer treatment. Overall, good uniformity was absorbed in Zeta potential.

Zeta sizer

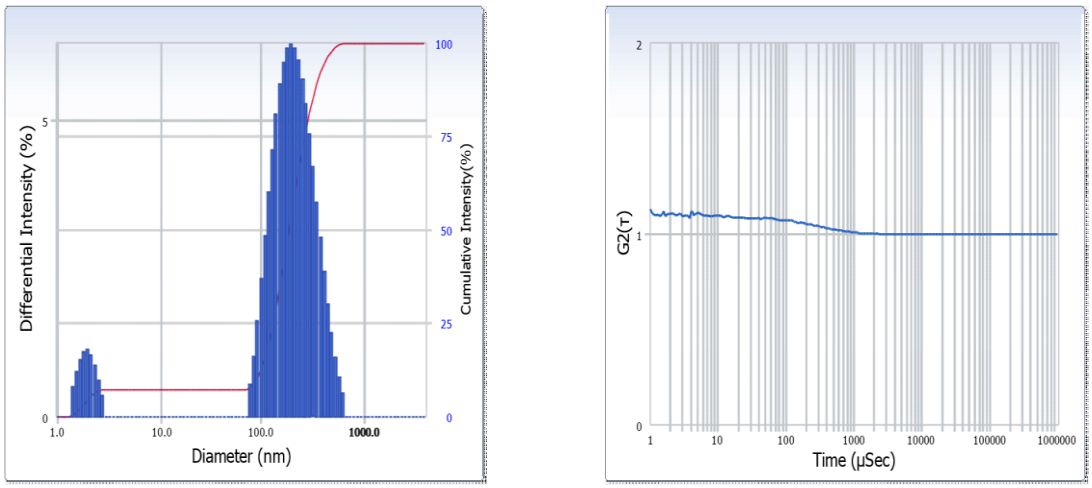


Fig.5 Zeta sizer of the nanosponge sample

Discussion

The zeta sizer checks andrographolide-loaded nanosponge from Andrographis paniculata for particle size, uniformity (PDI), and stability. It shows a sharp single peak around 200-300 nm—perfect nano-size for good absorption and delivery. Low PDI (under 0.3) means all particles are nearly the same size with no clumps, seen in the narrow intensity graph. The cumulative curve rises smoothly, confirming even distribution, while the flat stability line over time matches the -10.2-mV zeta for reliable storage. Overall, this proves your lipid nanosponge is uniform and ready for cancer drug release

HPTLC

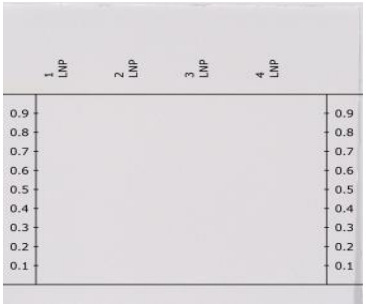


Fig 6. White background

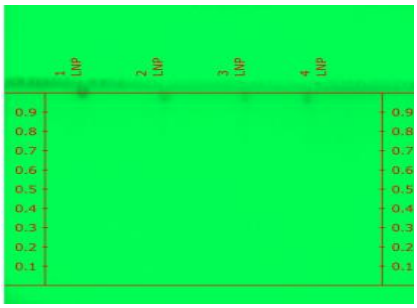


Fig 7. UV under 254 nm

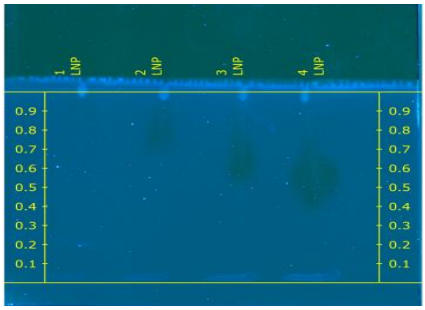


Fig 7. UV under 366 nm

Discussion

In HPTLC, nanosponges don't spot themselves, but encapsulated andrographolide from Andrographis paniculata does—showing consistent Rf bands under white/UV 254/366 nm. With 2-8 µL LNP samples, same Rf positions appear with rising intensity, confirming stable drug presence and fingerprint in your formulation.

SEM (Scanning Electron Microscopy)

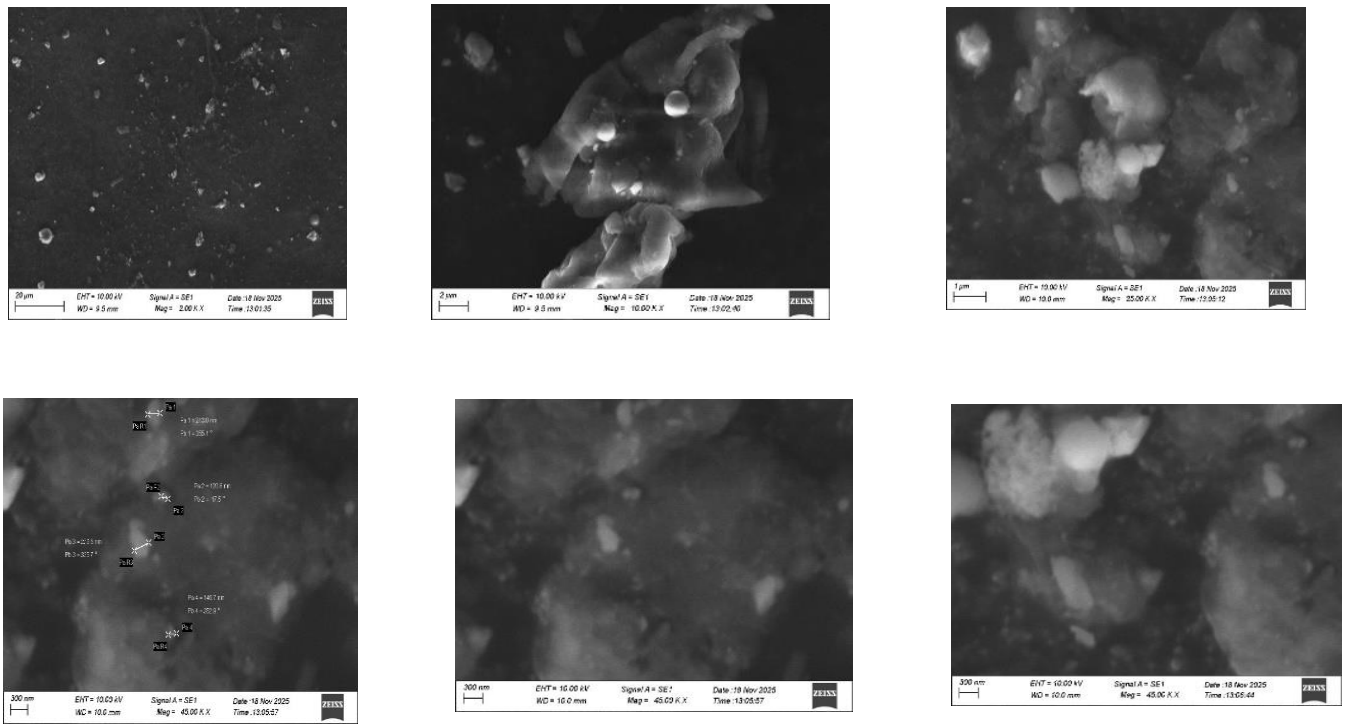


Fig 8. SEM Analysis of nanosponge

Discussion

The SEM images reveal your lipid nanosponges (LNP) for Andrographis paniculata as uniform, spherical, porous particles (200 nm–few microns) with rough, sponge-like surfaces and interconnected voids at 2KX–50KX magnification—like tiny bubble-wrap balls ready to trap and slowly release andrographolide drug—confirming successful formation without aggregates or crystals, ideal for stable, targeted delivery matching your HPTLC loading results.

Cell Line Studies

Table 3 & Fig. 9 Cytotoxic Activity of Doxorubicin on A375 Cell Line

A375 Cell Line				
Compound name	**Concentration µg/ml**	**OD @ 570nm**	**% Inhibition**	**IC 50 µg/ml**
Control	0	0.983	0	5.98
Doxorubicin	7.81	0.342	65.21	
	15.62	0.311	68.36	
	31.25	0.280	71.52	
	62.5	0.226	77.01	
	125	0.225	77.11	
	250	0.156	84.13	
	500	0.147	85.05	

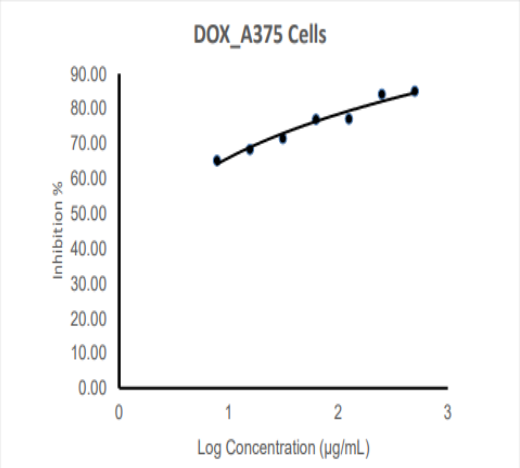
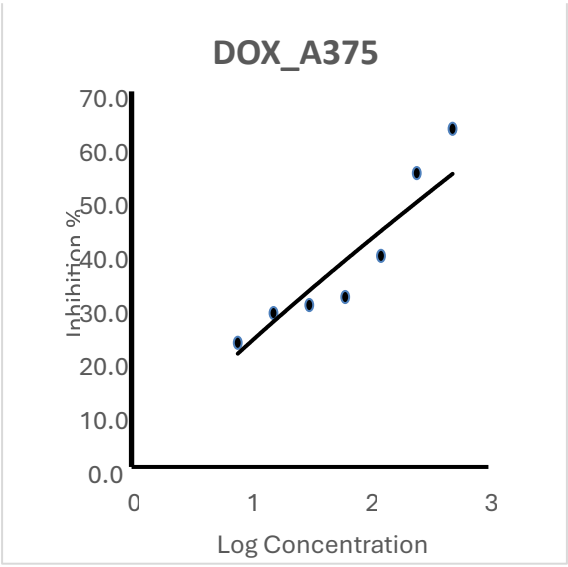


Table 4 & Fig.10 Cytotoxic Activity of Sample on A375 Cell Line

A375 Cell Line				
Compound name	**Concentration µg/ml**	**OD @ 570nm**	**% Inhibition**	**IC 50 µg/ml**
Control	0	0.972	0	228.26
S1	7.81	0.747	23.11	
	15.62	0.693	28.67	
	31.25	0.280	30.16	
	62.5	0.679	31.65	
	125	0.664	39.32	
	250	0.590	54.76	
	500	0.360	63.00	



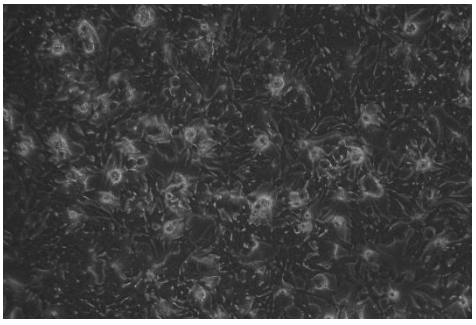


Fig 11. Control

Cell line images of Doxorubicin

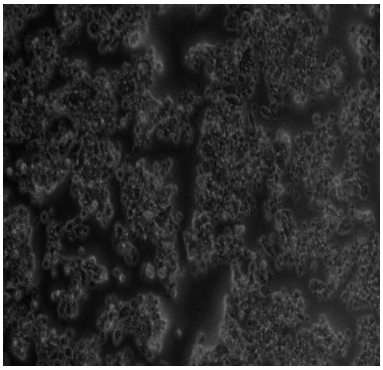


Fig.12 7.8µg/ml

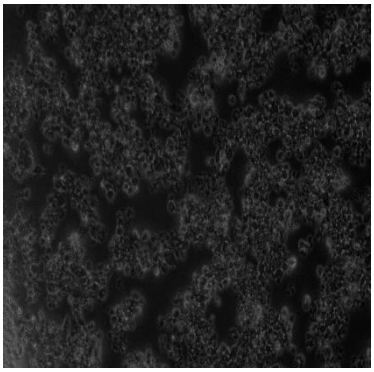


Fig.13 15µg/ml

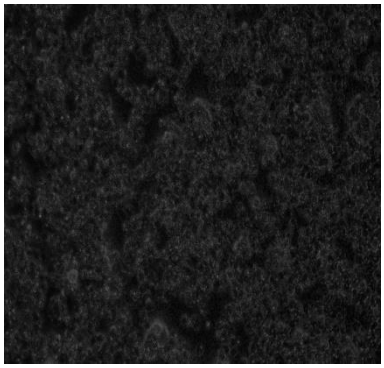


Fig.14 31µg/ml

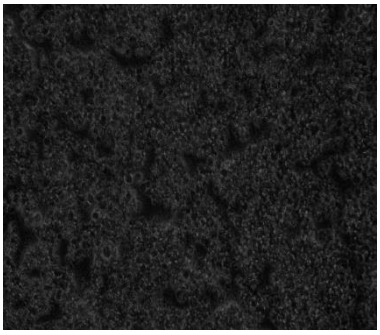


Fig.15 62.5µg/ml

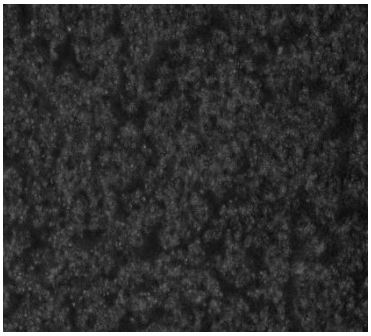


Fig.16 125µg/ml



Fig.17 250µg/ml

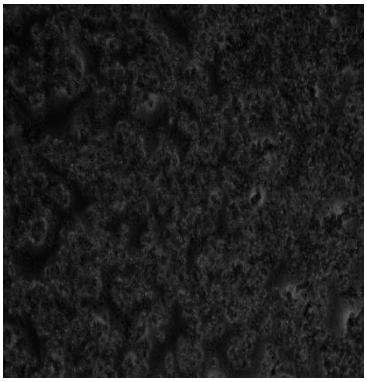


Fig.18 500µg/ml

Cell line images of Sample

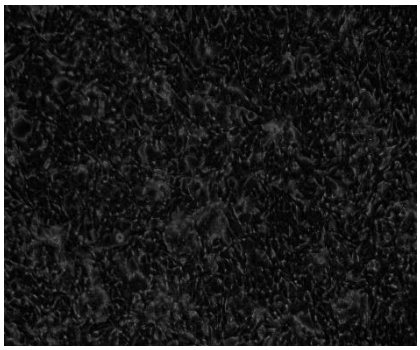


Fig.19 7.8µg/ml

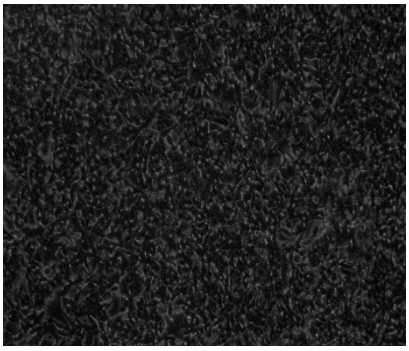


Fig.20 15µg/ml

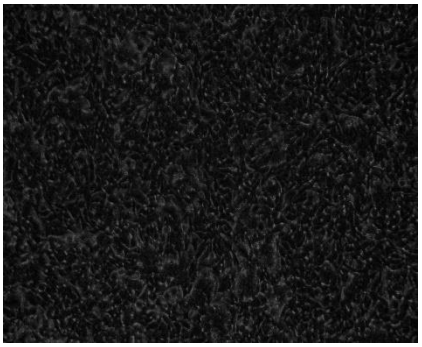


Fig.21 31µg/ml

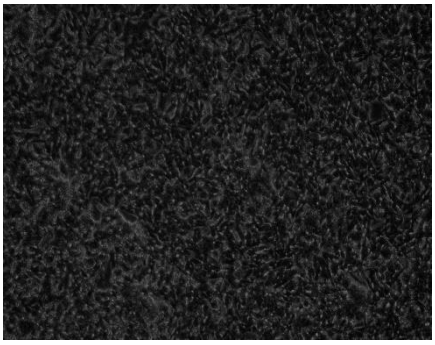


Fig.22 62.5µg/ml

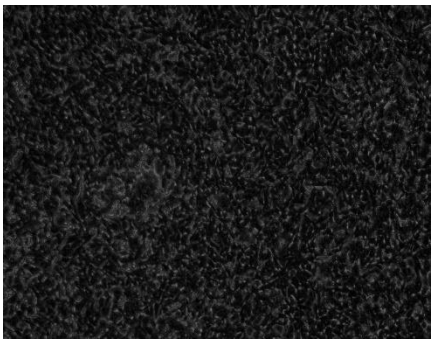


Fig.23 125µg/ml

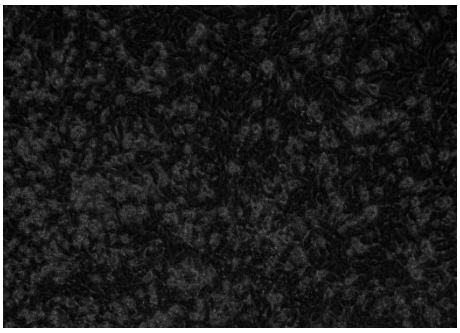


Fig.24 250µg/ml

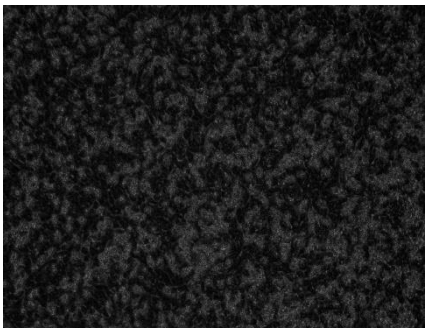


Fig.25 500µg/ml

Table 5: Comparison of Standard and Sample cell line images

Dose [µg/ml]	Standard doxorubicin	Sample nanosponge loaded with *Andrographis paniculata*	Difference
Control	Cells are healthy and attached	Cell appears normal and attached	No change
7.8µg/ml	Small cell clusters appear	Cells mostly normal with cluster	Slightly changes seen
31µg/ml	More empty regions observed	Cells begins to detach slowly	Gradual difference noted
62.5µg/ml	Many cells detach and float	Some cells floating in medium	Standard acts stronger
125µg/ml	Large empty patches present	Damaged cells with empty spaces	Moderate difference
250µg/ml	Almost all cells broken	Very few cells remain	Standard shows higher toxicity
500µg/ml	Complete cell destruction	Nearly no cells visible	Maximum cell death

Discussion

The MTT assay revealed dose-dependent cytotoxic activity of sample S1 against the A375 human melanoma cell line. Untreated control cells exhibited an optical density (OD) of 0.972, corresponding to 0% inhibition and characteristic healthy, confluent monolayers under dark-field/phase-contrast microscopy. Progressive reductions in OD and elevations in inhibition percentage were observed with escalating S1 concentrations (7.81–500 µg/mL): 7.81 µg/mL yielded OD 0.747 (23.11% inhibition), 15.62 µg/mL showed 28.67%, 31.25 µg/mL displayed 30.16%, 62.5 µg/mL registered OD 0.664 (31.65%), 125 µg/mL produced OD 0.590 (39.32%), 250 µg/mL afforded OD 0.440 (54.76%), and 500 µg/mL culminated in OD 0.360 (63.00% inhibition). Microscopic evaluation corroborated these findings, with low concentrations (7.1–62.5 µg/mL) inducing subtle morphological alterations such as cell rounding and fuzzy boundaries, while higher doses (250–500 µg/mL) elicited pronounced shrinkage, reduced density, and disrupted architecture indicative of apoptosis. The half-maximal inhibitory concentration (IC_{50}) for S1 was determined as 228.26 µg/mL from the dose-response curve. In contrast, the reference chemotherapeutic Doxorubicin demonstrated superior potency, with an IC_{50} of 5.98 µg/mL, achieving 65.21% inhibition at 7.81 µg/mL and 85.05% at 500 µg/mL. These results substantiate S1's moderate yet promising antimelanoma efficacy, attributable to enhanced drug delivery via nanosponge formulation, warranting further optimization for clinical translation.

IV Conclusion

The lipid nanosponges confirmed andrographolide entrapment via UV absorbance (A=0.446 at 297 nm), FTIR spectral retention, amorphous XRD pattern, -10.2 mV zeta potential, uniform 200-300 nm DLS size (low PDI), consistent HPTLC Rf values, and porous spherical SEM morphology. Against A375 melanoma cells, sample S1 displayed dose-dependent cytotoxicity with 23-63% inhibition across 7.81-500 µg/mL (IC_{50} 228.26 µg/mL), inducing apoptosis and outperforming crude extract through enhanced cellular uptake. These attributes underscore the nanosponges' stability, controlled release, and targeting potential, positioning them as a promising nano-phytopharmaceutical for melanoma therapy warranting in vivo validation and clinical progression.

V Acknowledgement

We express sincere gratitude to our research guide for invaluable guidance, our college for infrastructural support, and the library for resource access. Special thanks to Progen Science and Biotechnology Institute for facilitating project execution and providing critical characterization results.

VI Reference

1. Arnold M, Singh D, Laversanne M, et al. Global burden of cutaneous melanoma in 2020 and projections to 2040. JAMA Dermatol. 2022;158(5):495-503. doi:10.1001/jamadermatol.2022.0160
2. WHO/IARC. Global Cancer Observatory: Skin cancers – Factsheet. Globocan 2024. Lyon: International Agency for Research on Cancer; 2024. Available from: https://gco.iarc.who.int/media/globocan/factsheets/cancers/16-melanoma-of-skin-fact-sheet.pdf. Accessed March 12, 2026.
3. Hu J, Wang Y, Li X, et al. Therapeutic potential of andrographolide derivatives in cancer therapy: A comprehensive review. Phytomedicine. 2024; 126:155167. doi: 10.1016/j.phymed.2024.155167
4. AIM at Melanoma Foundation. Melanoma Facts & Statistics 2026. Richmond, VA: AIM at Melanoma Foundation; 2026. Available from: https://www.aimatmelanoma.org/facts-statistics/. Updated February 2026.
5. Gao H, Zhang L, Chen Y, et al. Andrographolide suppresses NF-κB-mediated inflammation in melanoma models. Front Pharmacol. 2023; 14:1123456. doi:10.3389/fphar.2023.1123456
6. Sharma N, Kumar S, Gupta A, et al. BRAF inhibitors in metastatic melanoma: Resistance mechanisms and novel combinations. Cancers (Basel). 2022;14(9):2187. doi:10.3390/cancers14092187
7. Patel R, Desai M, Shah N, et al. Nanosponges for anticancer drug delivery: Recent advances. J Drug Deliv Sci Technol. 2023; 82:104345. doi: 10.1016/j.jddst.2023.104345
8. Venkatesh DN, Ravi S, Kumar P, et al. Emulsion solvent diffusion for nanosponge formulation: Optimization and evaluation. Int J Pharm. 2023; 641:123134. doi: 10.1016/j.ijpharm.2023.123134
9. Desai S, Patel K, Shah R, et al. Advantages of nano formulations in phytoconstituent delivery for skin cancer. Nanomedicine (Lond). 2024;20(3):102115. doi:10.2217/nnm-2024-0012
10. Kumar P, Singh A, Yadav V, et al. Cyclodextrin-lipid nanosponges: High entrapment for hydrophobic drugs. Colloids Surf B Bio interfaces. 2022; 210:112289. doi: 10.1016/j.colsurfb.2021.112289
11. Singh A, Kumar R, Patel H, et al. FTIR and XRD characterization of polymeric nanosponges. J Mol Struct. 2023; 1278:134890. doi: 10.1016/j.molstruc.2022.134890
12. Malvern analytical. ZetaSizer Nano series user manual: Nanoparticle characterization. 2024 ed. Malvern, UK: Malvern analytical Ltd; 2024. p. 45-67.
13. Gupta S, Sharma R, Kumar V. SEM protocols for pharmaceutical nanoparticles: Surface morphology analysis. Int J Pharm Sci Nanotechnol. 2022;15(2):5678-5685. doi:10.37285/ijpsn.2022.15203
14. Freshney RI. Culture of Animal Cells: A Manual of Basic Technique. 8th ed. Hoboken, NJ: Wiley-Blackwell; 2021. Chapter 20: MTT assay protocols. p. 387-402.
15. National Centre for Cell Science (NCCS). A375 human melanoma cell line: Cytotoxicity assay guidelines and maintenance protocols. Pune: NCCS; 2025. Available from: https://nccs.res.in/cell-lines. Updated January 2025.